THE JOURNAL OF BIOLOGICAL CHEMISTRY VOL. 281, NO. 15, pp. 9996–10001, April 14, 2006

Dystrophin and Utrophin Bind Actin through Distinct Modes of Contact*

Received for publication, December 8, 2005, and in revised form, February 9, 2006 Published, JBC Papers in Press, February 13, 2006, DOI 10.1074/jbc.M513121200

Inna N. Rybakova, Jill L. Humston, Kevin J. Sonnemann, and James M. Ervasti[1]

From the Department of Physiology, University of Wisconsin Medical School, Madison, Wisconsin 53706

This study was designed to define the molecular epitopes of dystrophin-actin interaction and to directly compare the actin binding properties of dystrophin and utrophin. According to our data, dystrophin and utrophin both bound alongside actin filaments with submicromolar affinities. However, the molecular epitopes involved in actin binding differed between the two proteins. In utrophin, the amino-terminal domain and an adjacent string of the first 10 spectrin-like repeats more fully recapitulated the activities measured for full-length protein. The homologous region of dystrophin bound actin with low affinity and near 1:1 stoichiometry as previously measured for the isolated amino-terminal, tandem (CH) domain. In contrast, a dystrophin construct including a cluster of basic spectrin-like repeats and spanning from the amino terminus through repeat 17, bound actin with properties most similar to full-length dystrophin. Dystrophin and utrophin both stabilized preformed actin filaments from forced depolymerization with similar efficacies but did not appear to compete for binding sites on actin. We also found that dystrophin binding to F-actin was markedly sensitive to increasing ionic strength, although utrophin binding was unaffected. Although dystrophin and utrophin are functionally homologous actin-binding proteins, these results indicate that their respective modes of contact with actin filaments are markedly different. Finally, we reassessed the abundance of dystrophin in striated muscle using full-length protein as the standard and measured greater than 10-fold higher values than previously reported.

Dystrophin and utrophin are homologous proteins with similar interacting partners. By providing a link between the actin cytoskeleton and the extracellular matrix, dystrophin functions to maintain the integrity of the cell membrane during muscle contraction. Consequently, genetic ablation of dystrophin leads to increased fragility in the muscle membrane and results in the pathologies observed in Duchenne and Becker muscular dystrophies and some forms of cardiomyopathy. The functional role of utrophin is not completely understood. However, utrophin overexpression in the dystrophin-deficient *mdx* mouse has been shown to correct all known parameters of the dystrophic phenotype (1). Notably, utrophin overexpression rescued the mechanical linkage between costameric actin and the sarcolemma of the dystrophin-deficient *mdx* mouse muscle (2).

Like other members of the spectrin superfamily of proteins, both dystrophin and utrophin interact with actin via the amino-terminal tandem calponin homology (CH)[2] actin-binding domain (3–6). Additionally, in both dystrophin and utrophin, the spectrin-like repeats of the rod domain have been shown to contribute to actin binding. According to our recent study, the first 10 spectrin-like repeats of utrophin increase the affinity and capacity of its amino-terminal domain for actin (7). The actin binding activity of the homologous region of dystrophin has not been investigated yet. However, a cluster of basic repeats 11–17 of dystrophin was shown to bind actin independently of its amino-terminal domain (8). The homologous repeats in utrophin are acidic and exhibited no actin binding activity (8). In spectrin, a protein crucial for the stability of erythrocyte membranes, the very first repeat of the rod domain contributes to tandem CH domain association with actin (9). Actin-binding sites distributed throughout the amino-terminal and rod domains of spectrin, utrophin, and dystrophin create the extended contact with actin filament, consequently providing more effective mechanical stabilization of the cell membrane.

Evaluation of how much of the dystrophin rod domain is involved in association with actin is therefore of interest from many perspectives. First, it will contribute to the understanding of diverse actin-binding mechanisms, and how particular spectrin-like repeats are modified to serve different functional requirements of the proteins. Second, mapping the molecular epitopes involved in association with actin and side-by-side comparison of dystrophin and utrophin with regard to the actin binding activities of the proteins may aid in designing the optimal utrophin construct to replace dystrophin in muscle. The actin binding properties of full-length utrophin and a series of truncated constructs were detailed in our recent publication (7). The actin binding characteristics are also available for the isolated amino-terminal and middle rod domains of dystrophin, as well as full-length protein associated with the glycoprotein complex (3, 5, 8, 10, 11). However, the finding that α1-syntrophin, a component of the glycoprotein complex, binds actin prompts the evaluation of actin binding characteristics of dystrophin in the absence of any potential contribution by its associated proteins (12, 13).

In this study, we expressed full-length mouse dystrophin and characterized its actin binding properties by high speed sedimentation and PRODAN-labeled F-actin depolymerization assays. Using full-length dystrophin as a standard we measured the absolute dystrophin content in striated muscle of control mice at more than 10-fold greater than the dystrophin content of control muscle estimated previously (14). To define the molecular epitopes of dystrophin-actin interaction, we further generated two dystrophin fragments encoding the amino-terminal domain and 10 or 17 spectrin-like repeats. A side-by-side comparison of full-length dystrophin and utrophin and dystrophin fragments, lead us to conclude that dystrophin and utrophin are functionally homologous actin-binding proteins but act through distinct modes of contact.

* This study was supported by an American Heart Association Scientist development grant (to I. N. R.), American Heart Association Predoctoral Fellowship (to K. J. S.), and National Institutes of Health Grant ARO42423 (to J. M. E.). The costs of publication of this article were defrayed in part by the payment of page charges. This article must therefore be hereby marked "*advertisement*" in accordance with 18 U.S.C. Section 1734 solely to indicate this fact.

[1] To whom correspondence should be addressed: Dept. of Physiology, University of Wisconsin, 127 Service Memorial Institute, 1300 University Ave., Madison, WI 53706. Tel.: 608-265-3419; Fax: 608-265-5512; E-mail: ervasti@physiology.wisc.edu.

[2] The abbreviations used are: CH, calponin homology; Dys, dystrophin; Utr, utrophin.

EXPERIMENTAL PROCEDURES

Proteins—Full-length dystrophin was derived from the transgenic expression vector pMDA, encoding mouse dystrophin cDNA (15). The first 1.2 kb of dystrophin sequence was PCR-amplified from pMDA using the following set of primers (Integrated DNA Technologies) 5′-GCGGCCGCACCATGGACTACAAGGACGACGATGACAAG-CTTTGGTGGGAAGAA-3′and 5′-GCGCCCAACTAGTTGACTT-CCTAACTGTAGAACATTAC-3′. The forward primer was designed with the FLAG epitope (underlined) in-frame with the dystrophin coding sequence. The PCR product was sequenced and inserted into the EcoR1 and SpeI sites of pFastBac1 transfer plasmid (Invitrogen), producing the intermediate plasmid. A 12.5-kb SpeI fragment encoding the remaining 3′-portion of the dystrophin cDNA was excised from pMDA with SpeI and added into the intermediate plasmid to produce pFastBac1 vector encoding full-length mouse dystrophin with the amino-terminal FLAG epitope. A DNA fragment encoding the amino terminus and 10 or 17 spectrin-like repeats of dystrophin were PCR-amplified from the pFastBac1 vector containing the full-length mouse dystrophin sequence. The sequence-verified PCR products were ligated into pFastBac1 transfer plasmid. The resulting pFastBac1 vectors encoding full-length dystrophin and dystrophin fragments were used for the site-specific transposition of an expression cassette into bacmid. Baculovirus strains prepared from the recombinant bacmids were used to infect SF9 cell monolayers for dystrophin protein expression. Recombinant dystrophin proteins were isolated from infected insect cell lysates on anti-FLAG M2-agarose (Sigma) as previously described for the purification of full-length FLAG-tag utrophin (2). Full-length mouse utrophin was expressed in the baculovirus expression system as described previously (2). Lyophilized rabbit skeletal muscle actin was purchased from Cytoskeleton and reconstituted according to manufacturer's instructions.

Hydrodynamic Analysis—Measurements of the sedimentation coefficient and Stokes radius as well as the calculation of the native molecular weight and frictional coefficient of dystrophin proteins were performed as described previously (8, 16).

Actin Binding Analysis—The actin binding properties of dystrophin proteins were measured using the previously described high speed cosedimentation assay (5). Briefly, increasing amounts of purified protein incubated with 6 μM muscle F-actin were centrifuged at 100,000 × *g* for 20 min. The amount of free and bound protein was determined densitometrically from Coomassie Blue-stained gels of resulting supernatants and F-actin pellet fractions. Binding data were fitted to a hyperbolic binding equation by non-linear regression analysis (17).

PRODAN Actin Depolymerization Assay—PRODAN-labeled actin (18) was the kind gift of Dr. G. Marriott (University of Wisconsin, Madison, WI). PRODAN-actin filaments assembled alone or in the presence of dystrophin or utrophin were induced to depolymerize by dilution to 0.1 μM in low salt buffer conditions. Fluorescence measurements were performed at 25 °C in an SLM-AMINCO AB2 fluorescence spectrophotometer (ThermoElectron) at an excitation wavelength of 385 + 4 nm and an emission wavelength of 465 + 4 nm.

Quantitation of Dystrophin Protein Expression in Muscle—0.5 g of cardiac or skeletal muscle of C57BL/10 control mice (Jackson Laboratories, Bar Harbor, ME) were pulverized in a liquid nitrogen and solubilized in 2 ml of 1% SDS, 5 mM EGTA, and a mixture of protease inhibitors. The samples were incubated for 2 min at 100 °C and centrifuged at 12,000 × *g*. The protein concentration of the resulting supernatants was measured with Bio-Rad DC protein assay kit. Nitrocellulose transfers containing various loads of total protein were incubated with a 1:100 dilution of mAb Dys2 (Novocastra Laboratories, Newcastle, United Kingdom), and immunoreactivity was detected with ^{125}I-labeled goat anti-mouse IgG and autoradiography. A standard curve of purified recombinant dystrophin was included on transfers. The intensities of immune signal were analyzed densitometrically.

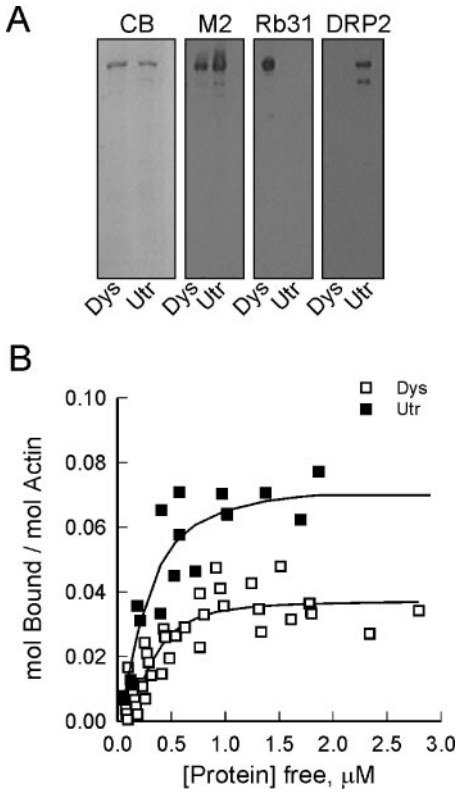

FIGURE 1. **Comparison of dystrophin and utrophin actin binding characteristics.** *A*, Coomassie Blue-stained SDS-PAGE (*CB*) and identical immunoblots containing Dys and Utr purified from infected SF9 cells. Immunoblots were stained with antibodies to FLAG epitope (*M2*), dystrophin (*Rb31*), and utrophin (*DRP2*). *B*, increasing amounts of Dys and Utr were cosedimented with F-actin at 100,000 × *g*. The amount of free and bound Dys and Utr was determined densitometrically from Coomassie Blue-stained SDS-PAGE loaded with equal volumes of resulting supernatants and pellets. *Symbols* denote the data from three independent experiments, and *lines* represent the fitted values.

TABLE 1
Physical properties of dystrophin proteins

Protein	DysN-R10	DysN-R17	Dys
Predicted M_r	170,241	258,188	427,797
Denatured M_r	168,537	245,094	396,641
Native M_r	177,368	232,106	441,867
Stokes radius, nm	6.6	7.5	9.7
Sedimentation coefficient, s	6.3	7.2	10.6
Frictional coefficient	1.76	1.84	1.92

RESULTS

We have previously characterized the actin binding properties of dystrophin in dystrophin-glycoprotein complex purified from rabbit skeletal muscle (5, 16). To examine the dystrophin/actin interaction in the absence of any potential contribution by its associated proteins and to directly compare dystrophin and utrophin actin binding activities, we expressed full-length mouse dystrophin in the baculovirus expression system as was previously described for utrophin (2). As for utrophin, dystrophin was designed with the FLAG epitope on its amino terminus and therefore purified on anti-FLAG M2-agarose (Fig. 1*A*). Gel filtration chromatography in combination with density gradient centrifugation revealed that purified dystrophin was composed of elongated monomers in the solution (Table 1). We further subjected increasing

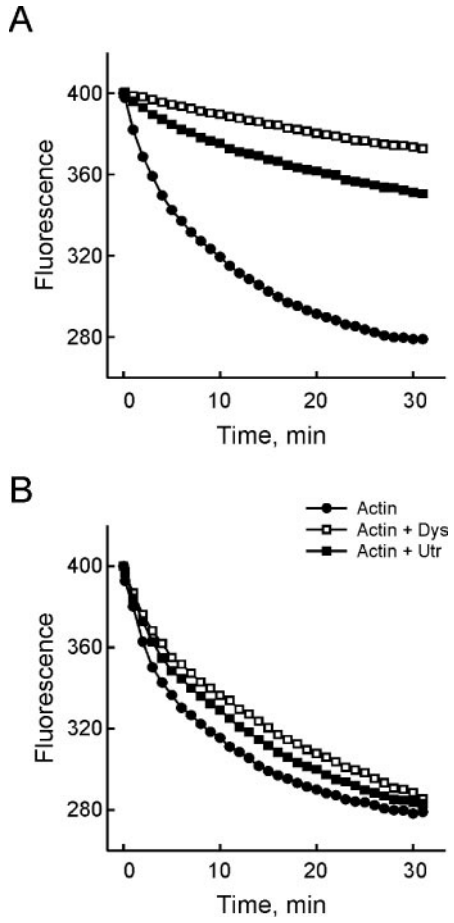

FIGURE 2. **Effect of dystrophin and utrophin on forced depolymerization of actin filaments.** 1 μM PRODAN-labeled F-actin was preincubated alone (*Actin*) or in the presence of dystrophin or utrophin. Depolymerization was monitored by measuring fluorescence of actin filaments decline after dilution to 0.1 μM into low salt buffer conditions. Graphs represent the results of typical experiments where the dystrophin/utrophin: actin molar ratio was 1:12 (*A*), or 1:24 (*B*).

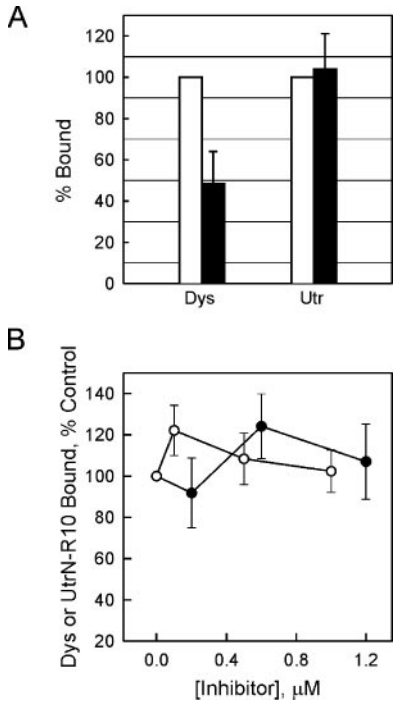

FIGURE 3. **Dystrophin and utrophin show different sensitivity to NaCl and do not compete for binding sites on F-actin.** *A*, dystrophin and utrophin at the K_d concentration was cosedimented with 6 μM F-actin in the presence of 0.1 M (*open bars*) or 0.5 M NaCl (*filled bars*). The binding data ($n = 3$; $\pm$S.D.) were normalized against amount of actin pelleted and expressed as the percentage of dystrophin and utrophin cosedimented with F-actin in 0.1 M NaCl. *B*, 6 μM F-actin was cosedimented with 0.5 μM Dys in the presence of increasing amounts of UtrN-R10, or 6 μM F-actin was cosedimented with 0.5 μM UtrN-R10 in the presence of increasing amounts of dystrophin. The amount of dystrophin (*open circles*) and UtrN-R10 (*filled circles*) bound to actin was determined densitometrically from Coomassie Blue-stained gels of the resulting supernatant and pellet fractions. Average data ($\pm$S.D., $n = 3$) were expressed as the percentage of Dys or UtrN-R10 pelleted with F-actin, where 100% equals 0.0134 $\pm$ 0.001 mol of dystrophin bound per mol of actin in the absence of UtrN-R10 and 0.0257 $\pm$ 0.003 mol of UtrN-R10 bound per mol of actin in the absence of Dys.

amounts of the purified protein to high speed cosedimentation with 6 μM F-actin. To directly compare dystrophin and utrophin with regard to the actin binding activity of each protein, the experiments were performed in parallel with full-length utrophin. Fitting the binding data obtained from three independent experiments to the hyperbolic binding equation showed that dystrophin and utrophin bound actin with similar K_ds of 0.32 $\pm$ 0.04 μM and 0.29 $\pm$ 0.1 μM, respectively (Fig. 1*B*). However, the B_{max} values for dystrophin (0.037 $\pm$ 0.003) and utrophin (0.077 $\pm$ 0.01) indicated that the proteins differed in extent of lateral association with actin. Thus, dystrophin appeared to occupy 27 $\pm$ 2 actin monomers on actin filament *versus* 13 $\pm$ 2 actin monomers bridged by utrophin. To analyze whether this difference made dystrophin more efficient in stabilizing actin filaments, we directly compared the effect of each protein on forced depolymerization of PRODAN-labeled F-actin. Considering the differences in B_{max} values, the experiments were performed at 1:12 and 1:24 molar ratios measured for saturable binding to actin for utrophin and dystrophin, respectively. PRODAN-labeled actin depolymerization analysis demonstrated that dystrophin and utrophin protected actin filaments with similar efficacies and that the protective effect was dependent on the dystrophin and utrophin:actin molar ratio. At 1 dystrophin or utrophin presented per every 12 actin monomers, the protective effect lasted over a wide time range (Fig. 2*A*). At 1:24 molar ratio, both proteins had a smaller effect on actin filament decay (Fig. 2*B*).

As we reported previously, utrophin binds actin via a continuous site composed of its amino terminus and a string of the first 10 spectrin-like repeats of the rod domain (7). It was therefore possible that spectrin repeats 1–10 of dystrophin also may contribute to its actin binding activity. Alternatively, dystrophin may bind actin through two distinct sites located on its amino terminus and middle rod domain. A recombinant dystrophin fragment corresponding to the middle rod domain of dystrophin and encoding a cluster of basic spectrin-like repeats 11–17 has been shown to bind actin in a NaCl-sensitive manner through an electrostatic interaction (8). Consistent with this observation, full-length dystrophin binding to actin decreased 50% in the presence of 0.5 M NaCl, whereas the utrophin-actin interaction was unaffected (Fig. 3*A*).

In view of the differences between dystrophin and utrophin actin binding properties, we further evaluated whether they compete for the binding sites on actin filaments. Because Dys and Utr are indistinguishable on Coomassie-Blue-stained gel (Fig. 1*A*) and because the utrophin fragment corresponding to the amino terminus of utrophin and 10 spectrin-like repeats of its rod domain (UtrN-R10) recapitulates the actin binding activity of full-length utrophin, we tested whether UtrN-R10 could inhibit dystrophin binding to actin. UtrN-R10 had no effect on dystrophin binding to actin, because the amount of dystrophin cosedimented with actin did not change over a range of UtrN-R10 concentrations (Fig. 3*B*). Similarly, dystrophin was found to have no effect on UtrN-R10 binding to actin (Fig. 3*B*).

To investigate how much of the dystrophin rod domain is necessary for high affinity binding measured for full-length dystrophin-actin

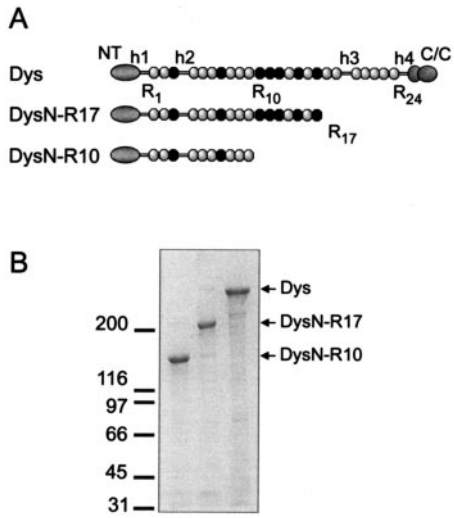

FIGURE 4. **Dystrophin constructs expressed in baculovirus system.** Shown in *A*, is a schematic representation of full-length dystrophin and recombinant dystrophin fragments (DysN-R10 and DysN-R17). *NT*, amino-terminal tandem CH domain; *h1–h4*, hinge regions; R_1–R_{24}, spectrin-like repeats region; *C/C*, cysteine-rich and carboxyl-terminal domains. Basic repeats are shaded in *black*. *B*, dystrophin constructs were designed with an amino-terminal FLAG epitope and purified from insect cell lysates on anti-FLAG M2-agarose. 25 μl of 1-ml peak fractions eluted with an excess of FLAG-peptide were subjected to SDS-PAGE and stained with Coomassie Blue. The molecular weight standards ($\times 10^{-3}$) are indicated on the left.

interaction, we generated two dystrophin fragments, DysN-R10 and DysN-R17 (Fig. 4). DysN-R10 was designed to correspond to the extended actin-binding site of utrophin (UtrN-R10) and therefore encoded the amino terminus of dystrophin and 10 spectrin-like repeats of its rod domain. DysN-R17 spanned from the amino terminus through the cluster of basic repeats 11–17 that display intrinsic actin binding activity (8). Hydrodynamic analysis showed that both proteins purified as soluble monomers of elongated shape (Table 1). Cosedimentation of DysN-R10 and DysN-R17 with F-actin demonstrated that both dystrophin fragments bound actin in a saturable manner yet with dramatically different properties (Fig. 5*A*). DysN-R10 bound actin with a K_d of 13.7 ± 7.1 μM (Fig. 5*B*), similar to that previously measured for the isolated amino-terminal tandem CH domain of dystrophin (10). In comparison, a K_d of 0.76 ± 0.39 μM, measured for DysN-R17 binding to actin, was comparable to the K_d value obtained for full-length Dys. The data shown in Fig. 5 strongly suggest that dystrophin requires a cluster of basic spectrin-like repeats to bind actin with high affinity and high capacity. The plots of K_d and B_{max} *versus* spectrin repeat number (Fig. 5, *B* and *C*) demonstrate that DysN-R10 lacking the cluster of basic repeats bound to actin with low affinity and a 1:1 stoichiometry analogous to the isolated amino-terminal tandem CH domain of dystrophin and further support the importance of repeats 11–17 for dystrophin-actin interaction.

We also made use of the purified full-length dystrophin as a standard to measure the absolute dystrophin content in the striated muscle of control mice by quantitative Western blot analysis (Fig. 6). Mouse skeletal and cardiac muscle exhibited similar dystrophin abundances of 0.026 ± 0.014% and 0.026 ± 0.003%, respectively. The value of dystrophin level in skeletal muscle measured in this study was more than 10-fold greater than the dystrophin content of cardiac muscle estimated previously (14).

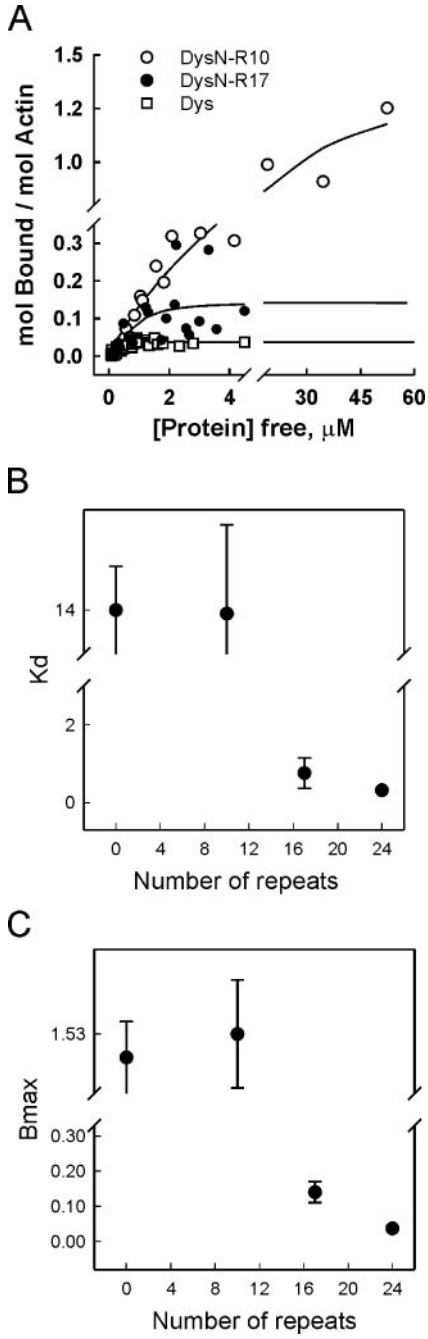

FIGURE 5. **Recombinant dystrophin constructs binding to F-actin.** *A*, increasing amounts of DysN-R10, DysN-R17, and full-length Dys were incubated with 6 μM F-actin and centrifuged at 100,000 × *g*. The amount of free and bound proteins was determined densitometrically from Coomassie Blue-stained SDS-PAGE loaded with equal volumes of resulting supernatants and pellets. *Symbols* denote the data from three independent experiments, and *lines* represent the fitted values. Values (n = 3; ±S.D.) for K_d (*B*) and B_{max} (*C*) calculated from the data in A were plotted against the number of spectrin-like repeats present with the amino-terminal domain. The data indicated for 0 repeats report the values for the isolated amino-terminal domain of dystrophin (Dys246) as measured previously (10).

DISCUSSION

Transgenic utrophin overexpression has been shown to correct all known phenotypic parameters associated with dystrophin deficiency in *mdx* mice (1). A widespread perception, however, is that utrophin levels must greatly exceed the content of dystrophin in normal muscle to effect full rescue from the dystrophic phenotype. We believe this perception is largely based on an early quantitative estimate (14) of dystrophin abundance in normal cardiac muscle (0.002% of total muscle protein) and our own measurements of utrophin expression (2) in normal (0.0006%) and *mdx* skeletal muscle (0.0013%), as well as in the Fiona line of transgenic *mdx* mice overexpressing utrophin to levels (0.014%) that

fully corrected the *mdx* phenotype (1). From these measurements, it can reasonably be concluded that up to 7-fold greater levels of utrophin (0.014/0.002%) may be necessary to compensate for dystrophin deficiency. However, a short 60-kDa dystrophin fragment was used as a standard to determine the expression level of 427-kDa full-length protein by Western blot analysis in the early measurement of dystrophin content in cardiac muscle (14). Although state-of-the-art at the time, the much smaller protein fragment likely transferred more efficiently than full-length dystrophin, raising concern that this measurement underestimated the content of dystrophin in cardiac muscle. Using full-length protein as a standard, we determined that dystrophin abundance in normal cardiac muscle (0.026 ± 0.003%) and skeletal muscle (0.026 ± 0.014%) was more than 10-fold greater than the previous estimate (0.002%). Our measurements more closely agree with the quantitation of dystrophin abundance (19) in highly purified sarcolemma vesicles (2%) and with estimates that sarcolemmal proteins comprise 1% of total muscle protein based on the abundance of sodium channels in total muscle homogenates and purified sarcolemmal vesicles (20). Most importantly, our data indicate that up-regulation of utrophin in *mdx* muscle (0.0013/0.026% = 5% of wild type dystrophin levels) is below the lowest level of transgenic dystrophin expression (20% of wild type) found to rescue the dystrophic phenotype (21). When utrophin expresses to levels approaching that of dystrophin in normal muscle (0.014/0.026% = 54%) as in the Fiona line of transgenic mice, it can fully rescue the *mdx* phenotype (1).

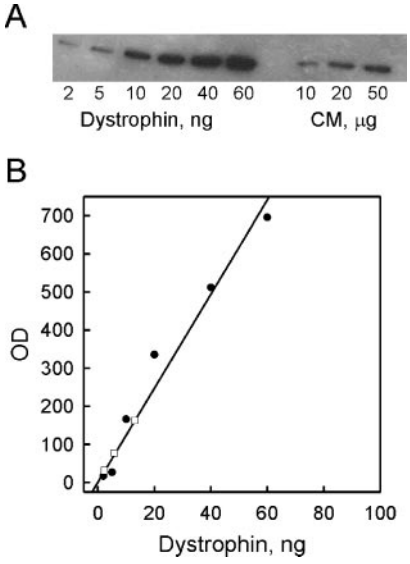

FIGURE 6. **Dystrophin protein abundance in striated muscle.** *A*, autoradiogram from a nitrocellulose transfer containing the various amounts of purified full-length dystrophin and cardiac muscle (*CM*) extract stained with Dys2 and detected by ^{125}I-labeled anti-mouse IgG. *B*, standard curve of autoradiographic intensity *versus* dystrophin load from the autoradiogram in *A*. The dystrophin signals obtained for different loads of cardiac muscle extract are indicated by *open squares*. The dystrophin content of 10, 20, and 50 μg of total protein loaded was 0.024, 0.029, and 0.026%, respectively. The average dystrophin content in cardiac muscle was 0.026 ± 0.003%. The average dystrophin content in skeletal muscle determined by the same method (not shown) was 0.026 ± 0.014%.

The direct comparison of actin binding properties of dystrophin and utrophin demonstrated that they are functionally interchangeable. First, both proteins bound actin with similar submicromolar affinities (Fig. 1*B*). Second, although a significantly higher B_{max} value measured for utrophin/actin interaction implies that utrophin bridges less actin monomers, forced depolymerization of preformed PRODAN-labeled actin filaments demonstrated that dystrophin and utrophin inhibited actin disassembly in a similar fashion (Fig. 2). One difference between dystrophin and utrophin, however, is the molecular epitopes involved in interaction with actin. As we demonstrated previously, the first 10 spectrin-like repeats of utrophin failed to bind actin (7). However, their presence in cis with the amino-terminal domain is necessary for the full actin binding activity of utrophin (Fig. 7). Although the equivalent region of dystrophin did not alter the actin binding properties of the adjacent amino-terminal domain, the addition of the repeats 11–17 to the DysN-R10 increased the affinity for actin almost 18-fold and provided more widely spaced distribution of dystrophin along the actin filament (Figs. 5 and 7). The dramatic changes in K_d and B_{max} values with the addition of repeats 11–17 to DysN-R10 argue for the necessity of this region of rod domain for the full actin binding activity measured for dystrophin. The salt sensitivity of dystrophin-actin interaction further validates the importance of spectrin-like repeats 11–17 for dystrophin actin binding activity. Indeed, this region of the dystrophin rod domain represents a cluster of basic repeats (Fig. 7) and was shown to bind actin via electrostatic interaction (8). Here, we showed that full-length dystrophin binding to actin was ~50% abolished in the presence of 0.5 M NaCl (Fig. 3*A*). Dystrophin-glycoprotein complex cosedimentation with F-actin was also found to be sensitive to increasing NaCl concentrations, and was about 40% inhibited in 0.5 M NaCl (5). Interestingly, the dystrophin-glycoprotein complex and full-length recombinant dystrophin bound actin with similar K_d and B_{max} values (Fig. 7). These results suggest that neither α1-syntrophin, or any other dystrophin-associated protein contributed to the actin binding characteristics previously measured for native dystrophin-glycoprotein complex (5). A considerable amount of syntrophins is recovered in the soluble fraction after muscle homogenization (13) and does not copurify with the dystrophin-glycoprotein complex (22). Furthermore, the soluble syntrophins were shown to be able to interact with actin and inhibit actin binding to myosin. These findings, in combination with our results, lead us to suggest

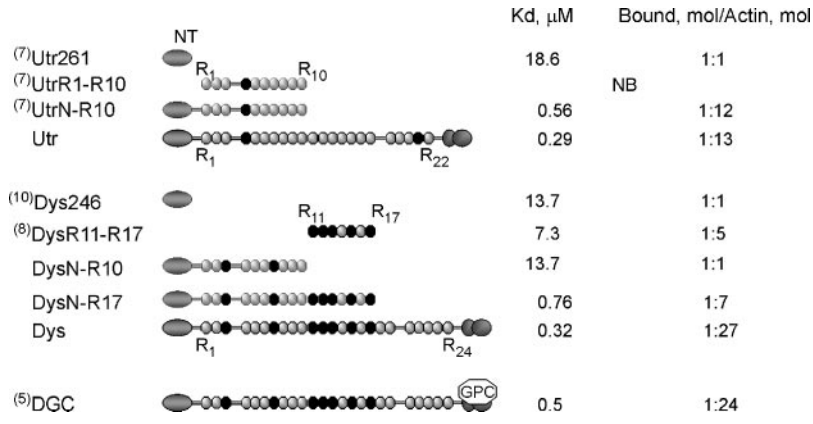

FIGURE 7. **Actin binding properties of dystrophin and utrophin proteins.** Shown is a schematic representation of utrophin (Utr261, UtrR1-R10, UtrN-R10, Utr) and dystrophin (Dys246, DysR11-R17, DysN-R10, DysN-R17, Dys) proteins, as well as dystrophin associated with the glycoprotein complex (*GPC*). *NT*, amino-terminal tandem CH domain; R_1–R_{24}, spectrin-like repeats of the rod domain. Basic repeats are shaded *black*. The actin binding properties (K_d and stoichiometry) of each protein are summarized on the right. *NB*, no measurable binding was observed. Utrophin and dystrophin proteins were described in this study or as indicated with the superscript.

that dystrophin and actin binding activities of syntrophins could be mutually exclusive.

The actin binding data obtained for the native dystrophin-glycoprotein complex, various dystrophin fragments, and for full-length protein fit well to the model in which dystrophin binds laterally along an actin filament through the concerted effect of two distinct low affinity binding sites. In contrast, utrophin interacts with multiple actin monomers via a single contiguous actin binding domain spanning from the amino terminus through repeat 10 of the rod domain (Fig. 7). The rod domains are the least conserved regions (35%) between dystrophin and utrophin (23), which may give rise to different modes of actin binding by spectrin-like repeats. In contrast, the amino-terminal tandem CH domains of dystrophin and utrophin are 80% identical (24) and were found to bind actin similarly (Fig. 7). Interestingly, different modes of contact were also shown for the interaction of cysteine rich/carboxyl-terminal domains of dystrophin and utrophin with β-dystroglycan (25). Although the cysteine-rich/carboxyl-terminal domains are 88% homologous between the two proteins, the regions involved in β-dystroglycan interaction were found to be only 66% similar (24). Lastly, we did not observe any effect of dystrophin on utrophin interaction with actin and vice versa (Fig. 3*B*). This finding suggests that both proteins could bind the same actin filament *in vivo*, supplementing one another. Although dystrophin and utrophin are expressed in muscle in a mutually exclusive manner, both proteins are present at the sarcolemma during the short period of neonatal development when dystrophin replaces utrophin (26–28). The noncompetitive actin binding via different modes of contact may therefore serve to protect the sarcolemma of increasingly active muscle from mechanical injuries during this transitional stage.

The rod domain of dystrophin is frequently speculated to function as a molecular spring or shock absorber. However, the molecular basis for these functions has not been proposed. We hypothesize that the two independent actin-binding sites employed by dystrophin may hold important clues to its mechanical function *in vivo*. For example, Wachsstock *et al.* (29) have demonstrated that multiple, rapidly rearranging cross-links can explain the loading rate-dependent, viscoelastic properties of actin filaments cross-linked by α-actinin. Likewise, the presence of two low affinity binding sites (likely binding and unbinding very rapidly) may enable the F-actin/dystrophin/sarcolemma linkage to respond elastically to rapid muscle stretches while yielding in a more fluid manner under prolonged strains of substantially lower magnitude (during muscle cell growth, or osmotic cell swelling with exercise, for example). Assuming that some portions of the dystrophin rod domain function as elastic elements, the cluster of actin-binding, basic rod domain repeats could act as a molecular "shock absorber" to dampen elastic recoil during contraction or stretch. In this role, the electrostatic binding of the dystrophin middle rod domain would be less sensitive (relative to a classical "lock and key" ligand/receptor interaction) to changes in binding interface orientation that would likely occur with its extension during muscle stretch. In contrast, our data indicate that utrophin lacks the basic middle rod domain and therefore also the capacity to function as a shock absorber. Given its single contiguous actin binding domain spanning from the amino terminus through repeat 10 (7) and its high expression during embryonic/fetal development, we hypothesize that utrophin may normally function as a molecular ruler to help define the length of costameric actin filaments during muscle development. The availability of full-length dystrophin and utrophin through expression in the baculovirus system now makes possible studies to characterize the mechanical properties of each protein through single molecule analyses (30).

Acknowledgments—We thank Dr. Jeffrey Chamberlain for the full-length mouse dystrophin cDNA (pMDA) and Dr. Gerard Marriott for providing PRODAN-labeled actin, access to his fluorescence spectrophotometer, and helpful discussions.

REFERENCES

1. Tinsley, J., Deconinck, N., Fisher, R., Kahn, D., Phelps, S., Gillis, J. M., and Davies, K. (1998) *Nat. Med.* **4,** 1441–1444
2. Rybakova, I. N., Patel, J. R., Davies, K. E., Yurchenco, P. D., and Ervasti, J. M. (2002) *Mol. Biol. Cell* **13,** 1512–1521
3. Way, M., Pope, B., Cross, R. A., Kendrick-Jones, J., and Weeds, A. G. (1992) *FEBS Lett.* **301,** 243–245
4. Winder, S. J., Hemmings, L., Maciver, S. K., Bolton, S. J., Tinsley, J. M., Davies, K. E., Critchley, D. R., and Kendrick-Jones, J. (1995) *J. Cell Sci.* **108,** 63–71
5. Rybakova, I. N., Amann, K. J., and Ervasti, J. M. (1996) *J. Cell Biol.* **135,** 661–672
6. Moores, C. A., and Kendrick-Jones, J. (2000) *Cell Motil. Cytoskeleton* **46,** 116–128
7. Rybakova, I. N., and Ervasti, J. M. (2005) *J. Biol. Chem.* **280,** 23018–23023
8. Amann, K. J., Guo, W. X. A., and Ervasti, J. M. (1999) *J. Biol. Chem.* **274,** 35375–35380
9. Li, X., and Bennett, V. (1996) *J. Biol. Chem.* **271,** 15695–15702
10. Renley, B. A., Rybakova, I. N., Amann, K. J., and Ervasti, J. M. (1998) *Cell Motil. Cytoskeleton* **41,** 264–270
11. Amann, K. J., Renley, B. A., and Ervasti, J. M. (1998) *J. Biol. Chem.* **273,** 28419–28423
12. Iwata, Y., Pan, Y., Yoshida, T., Hanada, H., and Shigekawa, M. (1998) *FEBS Lett.* **423,** 173–177
13. Iwata, Y., Sampaolesi, M., Shigekawa, M., and Wakabayashi, S. (2004) *Eur. J. Cell Biol.* **83,** 555–565
14. Hoffman, E. P., Brown, R. H., and Kunkel, L. M. (1987) *Cell* **51,** 919–928
15. Cox, G. A., Cole, N. M., Matsumura, K., Phelps, S. F., Hauschka, S. D., Campbell, K. P., Faulkner, J. A., and Chamberlain, J. S. (1993) *Nature* **364,** 725–729
16. Rybakova, I. N., and Ervasti, J. M. (1997) *J. Biol. Chem.* **272,** 28771–28778
17. Brooks, S. P. J. (1992) *BioTechniques* **13,** 906–911
18. Marriott, G., Zechel, K., and Jovin, T. M. (1988) *Biochemistry* **27,** 6214–6220
19. Ohlendieck, K., Ervasti, J. M., Snook, J. B., and Campbell, K. P. (1991) *J. Cell Biol.* **112,** 135–148
20. Barchi, R. L., and Weigele, J. B. (1979) *J. Physiol.* **295,** 383–396
21. Phelps, S. F., Hauser, M. A., Cole, N. M., Rafael, J. A., Hinkle, R. T., Faulkner, J. A., and Chamberlain, J. S. (1995) *Hum. Mol. Genet.* **4,** 1251–1258
22. McDearmon, E. L., Combs, A. C., and Ervasti, J. M. (2001) *J. Biol. Chem.* **276,** 35078–35086
23. Pearce, M., Blake, D. J., Tinsley, J. M., Byth, B. C., Campbell, L., Monaco, A. P., and Davies, K. E. (1993) *Hum. Mol. Genet.* **2,** 1765–1772
24. Tinsley, J. M., Blake, D. J., Roche, A., Byth, B. C., Knight, A. E., Kendrick-Jones, J., Suthers, G. K., Love, D. R., Edwards, Y. H., and Davies, K. E. (1992) *Nature* **360,** 591–593
25. Ishikawa-Sakurai, M., Yoshida, M., Imamura, M., Davies, K. E., and Ozawa, E. (2004) *Hum. Mol. Genet.* **13,** 693–702
26. Clerk, A., Strong, P. N., and Sewry, C. A. (1992) *Development* (*Camb.*) **114,** 395–402
27. Clerk, A., Morriss, G. E., Dubowitz, V., Davies, K. E., and Sewry, C. A. (1993) *Histochem. J.* **25,** 554–561
28. Radojevic, V., and Burgunder, J. M. (2000) *Cell Tissue Res.* **300,** 447–457
29. Wachsstock, D. H., Schwarz, W. H., and Pollard, T. D. (1993) *Biophys. J.* **65,** 205–214
30. Rief, M., Pascual, J., Saraste, M., and Gaub, H. E. (1999) *J. Mol. Biol.* **286,** 553–561